

MEASUREMENT OF FLUORESCENCE LIFETIMES USING MINIMUM NORM AND MULTIPARAMETER DECONVOLUTION

By

Abdussamad U. Jibia

Department of Mechatronics Engineering,

Bayero University Kano

ajumar@buk.edu.ng**ABSTRACT**

A new method of fluorescence decay analysis is presented. The method relies on the classical Gardner transform to convert the fluorescence decay data into a convolution model which is deconvolved using multiparameter deconvolution technique. Minimum norm eigenvector method is then used to further model the resulting complex exponentials to obtain better estimates of fluorescence decay rates and number of components. Simulation results indicate that the SNR detection threshold is very low compared with several other methods. Fluorescence decay data is finally post processed using the proposed approach.

Keywords: fluorescence, Gardner transform, multi-exponential, multi-parameter deconvolution, minimum norm.

INTRODUCTION

Fluorescence occurs when a molecule absorbs photons from the ultraviolet visible spectrum causing transition to a high energy electronic state and then emits photons as it returns to its initial state. While normal fluorescence spectroscopy is useful as a highly selective and non-invasive probe, better chemical information can be gained by exploiting the time-dependant nature of the fluorescence. This is referred to as time-resolved fluorescence spectroscopy (Lackowicz, 2006).

Time-resolved fluorescence provides more information about the molecular environment of the fluorophore than steady state fluorescence measurements. Since the fluorescence lifetime of a molecule is very sensitive to its molecular environment, measurement of the fluorescence lifetime(s) reveals much about the state of the fluorophore. Many macromolecular events, such as rotational diffusion,

resonance-energy transfer, and dynamic quenching, occur on the same time scale as the fluorescence decay. Thus, time-resolved fluorescence spectroscopy can be used to investigate these processes and gain insight into the chemical surroundings of the fluorophore.

There are two widely-used techniques in time-resolved fluorescence, viz. phase fluorometry and time-correlated single photon counting (TCSPC). In TCSPC which works well even for very small concentration of fluorophores the probe is excited by a continuous and periodic train of short pulses. The arrival time of a single photon is measured with respect to the last exciting light pulse. The procedure is repeated a large number of times and the record of arrival times kept. The task is then to derive fluorescent decay characteristic with the help of appropriate deconvolution and fitting procedure.

The observed fluorescent intensity $f(t)$ is related to the actual decay curve $I(t)$ by the integral equation:

$$f(t) = \int_{-\infty}^t I(t-T)G(T)dT \quad (1)$$

$G(T)$, is the instrument response function which contains information about the laser excitation and the time characteristics of the measurement system, i.e. the fluorimeter. The lower limit of is due to the assumption that the system is excited by an infinite and continuous train of laser pulses. $G(T)$, is periodic with a period

$$I(t) = \sum_{i=1}^M A_i \exp(-t/T_i) \quad (2)$$

Where $A_i, T_i, i = 1, 2, \dots, M$ are the parameters of the fluorescence decay curve. A_i are called preexponential factors while T_i are the lifetimes.

Eqn (2) can be more conveniently rewritten as:

$$I(t) = \sum_{i=1}^M A_i \exp(-\lambda_i t) \quad (3)$$

where $\lambda_i = 1/T_i, i = 1, 2, \dots, M$ are the decay rates.

A close examination of equations (2) and (3) would reveal that $I(t)$ is exactly the transient multi-exponential signal reviewed in Istratov & Vyvenko (1999) and Jibia & Salami (2012). Fluorescence decay is just one of the several sources of this class of signals and of the many methods reported for analyzing multi-exponentials, a few have been used for fluorescence decay analysis. These include the method of moments (Isenberg & Dyson, 1969), least squares (Isenberg, 1983), etc.

In this paper, an approach using a combination of multi-parameter deconvolution and minimum norm is presented. The two methods have been used separately for transient multi-exponential signal analysis. In Jibia et al (2008), multi-parameter deconvolution was used with MUSIC and minimum norm was used elsewhere with optimal compensation deconvolution (Jibia & Salami, 2007). The combination of minimum norm and multi-parameter deconvolution as presented in this paper is

equal to the repetition time of the excitation. If $f(t)$ and $G(T)$ contain statistical errors, which is usually the case, the solution to (1) becomes ill-posed. For most systems, the decay curve can be represented by a superposition of exponentials:

therefore new.

In section II, Gardner transform is used to convert the original signal into a convolution model which is discretized using the sampling procedure proposed in Jibia et al (2010). Multi-parameter deconvolution is then introduced in section III. In section IV the minimum norm method is introduced as applied to the deconvolved data. Simulation results are presented in section V. Section VI gives the experimental results. Finally, conclusion is given in section VII.

MPD/MINIMUM NORM COMBINATION

In this section, Gardner transform is applied to convert the signal in (3) into a convolution model hence removing the nonorthogonality problem associated with the signal.

Eq (3) can be expressed as follows:

$$I(\ddagger) = \int_0^\infty g(\}) \exp(-\}) \ddagger d\} \tag{4}$$

where

$$g(\}) = \sum_{i=1}^M A_i u(\} - \}_i) \tag{5}$$

The integral in Eq. (4) belongs to the more general class of Fredholm integral of the first kind which are known to be ill-posed. This term means that the solution of Eq. (4) may not be unique, may not exist, and may not depend continuously on the data.

Multiplying both sides of (4) by \ddagger^r , $r > 0$ and applying the Gardner transform [8], $\ddagger = e^t$ and $\} = e^{-t}$ results in the convolution integral

$$y(t) = \int_{-\infty}^\infty x(\}) h(t - \}) d\} \tag{6}$$

where

$$y(t) = \exp(rt) I(\exp(t)) \tag{7a}$$

$$x(t) = \exp((r - 1)t) g(e^{-t}) \tag{7b}$$

$$h(t) = \exp(rt) \exp(-e^{-t}) \tag{7c}$$

This is now a standard deconvolution problem in which $x(t)$ is the unknown input signal consisting of a series of weighted delta functions, $h(t)$ is the impulse

response and $y(t)$ is the output observation.

It can be shown [9] that the unknown input distribution function is given by

$$x(t) = \sum_{i=1}^M B_i u(t + \ln \}_i) \tag{8}$$

where $B_i = A_i(\}_i)^{-r}$

Eq. (6) can be converted to a discrete-time deconvolution model by sampling $y(t)$ at the rate of $f_s = 1/\Delta t$. This yields

$$y[n] = \sum_{m=n_{\min}}^{n_{\max}} x[m] h[n - m] \tag{9}$$

where $N = n_{\max} - n_{\min} + 1$ and the sampling interval is $\Delta t \leq \frac{1}{r}$.

Deconvolution of the convolution sum of Eq. (9) is achieved by solving stabilized solutions of integral of the first kind.

$$\int_{\Lambda_1}^{\Lambda_2} x(\tau)h(t, \tau)d\tau = Hx = y(t) \quad \text{for } T_1 < t < T_2 \quad (11)$$

We now select a space $F = W_2^q[\Lambda_1, \Lambda_2]$ and compute the square of the integrable functional form with derivatives of q order in the region of $[\Lambda_1, \Lambda_2]$.

The stable solutions \hat{x} should make the following smoothing functional a minimum:

$$M^s[\hat{x}, y] = \|H\hat{x} - y\|^2 + s\Omega(\hat{x}) \quad (12)$$

where $M^s[\hat{x}, y]$ expresses smoothing function.

Now, if we take the stable functional

$$\Omega(\hat{x}) = \int_{\Lambda_1}^{\Lambda_2} \sum_{r=0}^q \xi_r (d^r \hat{x})^2 d\tau \quad (13)$$

where ξ_r are selected known constants or functions of λ such that

$$\xi_r \geq 0 \quad \text{when } r = 0, 1, \dots, q-1$$

$$\text{and } \xi_q > 0 \quad \text{when } r = q$$

and $d^r \hat{x}$ is the expression of r^{th} order derivative of \hat{x} .

$$\begin{aligned} M^s[\hat{x}, y] &= \|H\hat{x} - y\|^2 + s\Omega(\hat{x}) \\ &= \|H\hat{x} - y\|^2 + s \int_{\Lambda_1}^{\Lambda_2} \sum_{r=0}^q \xi_r (d^r \hat{x})^2 d\tau \end{aligned} \quad (14)$$

In discrete form, this becomes

$$\begin{aligned} SM^s[\hat{x}(n), y(n)] &= \sum_{n=0}^{N-1} \left[y(n) - \sum_{m=-n_{\min}}^{n_{\max}} h(m)\hat{x}(n-m) \right]^2 \\ &\quad + s \sum_{r=0}^q \sum_{n=0}^{N-1} \xi_r \left[\sum_{m=-n_{\min}}^{n_{\max}} \nabla^r \hat{x}(n-m) \right]^2 \end{aligned} \quad (15)$$

where S denotes the sampling operation and ∇^r denotes the r^{th} order backward difference operator since ∇ is the discrete analog of the derivative.

In the frequency domain:

$$SM^s [\hat{X}(k), Y(k)] = \frac{\Delta t}{N} \sum_{k=0}^{N-1} |Y(k) - H(k)\hat{X}(k)|^2 + \frac{\Delta t}{N} \sum_{r=0}^q \sum_{k=0}^{N-1} \langle_r |L_r(k)\hat{X}(k)|^2 \tag{16}$$

Thus,

$$SM^s [\hat{X}(k), Y(k)] = \left\{ \begin{aligned} & \left[\begin{array}{l} Y(k) - H(k)\hat{X}(k) \\ Y^*(k) \\ -H^*(k)\hat{X}^*(k) \end{array} \right] \\ & + \sum_{r=0}^q \langle_r L(k) L^*(k)\hat{X}(k)\hat{X}^*(k) \end{aligned} \right\} \\ = \frac{\Delta t}{N} \sum_{k=0}^{N-1} \left\{ \begin{aligned} & Y(k)Y^*(k) - \\ & Y(k)H^*(k)\hat{X}^*(k) \\ & - H(k)\hat{X}(k)Y^*(k) \\ & + H(k)H^*(k) \\ & \hat{X}(k)\hat{X}^*(k) \\ & + \sum_{r=0}^q \langle_r L(k) L^*(k)\hat{X}(k)\hat{X}^*(k) \end{aligned} \right\} \tag{17}$$

$$\frac{\partial SM^s [\hat{X}(k), Y(k)]}{\partial \hat{X}(k)} = \left\{ \begin{aligned} & |H(k)|^2 X^*(k) \\ & - Y^*(k)H(k) \\ & + \sum_{r=0}^q \langle_r |L_r(k)|^2 \hat{X}^*(k) \end{aligned} \right\} \tag{18}$$

If $\frac{\partial SM^s [\hat{X}(k), Y(k)]}{\partial \hat{X}(k)} = 0$, then

$$\hat{X}^*(k) = \frac{Y^*(k)H(k)}{|H(k)|^2 + s \sum_{r=0}^q \langle_r |L_r(k)|^2} \tag{19}$$

Taking the complex conjugate of both sides yields

$$\hat{X}(k) = \frac{Y(k)H^*(k)}{|H(k)|^2 + \sum_{r=0}^q u_r |L_r(k)|^2} \tag{20}$$

$k = 0,1,2,\dots,N - 1$ and $u_r = s \langle_r$.

The term $|L_r(k)|^2$ is derived as follows:

From equation (15), let

$$b_r(n) = \nabla^r x[n] \tag{21}$$

Then, for $r = 1$

$$b_1(n) = \nabla x(n) = x(n) - x(n - 1) \tag{22}$$

So that

$$B_1(e^{j\check{s}}) = X(e^{j\check{s}})(1 - e^{j\check{s}}) \tag{23}$$

$$\text{Let } L_1(e^{j\check{s}}) = \frac{B_1(e^{j\check{s}})}{X(e^{j\check{s}})} = (1 - e^{j\check{s}}) \tag{24}$$

For DFT/FFT analysis

Taking $\check{S}_k = \frac{2fk}{N}$ yields

$$L_1(k) = 1 - e^{-j\frac{2fk}{N}} = 2j \sin \frac{fk}{N} e^{-j\frac{2fk}{N}} \tag{25}$$

$$\Rightarrow |L_1(k)|^2 = 4 \sin^2 \left(\frac{fk}{N} \right) \tag{26}$$

Similarly, for $r = 2$

$$L_2(e^{j\check{s}}) = \frac{B_2(e^{j\check{s}})}{X(e^{j\check{s}})} = -4e^{-j\check{s}} \left(\frac{e^{\frac{j\check{s}}{2}} - e^{-\frac{j\check{s}}{2}}}{2j} \right)^2 \tag{27}$$

With $\check{S} = \frac{2fk}{N}$, we have

$$L_2(k) = -4e^{-j\frac{2fk}{N}} \left(\sin^2 \left(\frac{fk}{N} \right) \right) \tag{28}$$

Hence,

$$|L_2(k)|^2 = 16 \sin^4\left(\frac{fk}{N}\right) \tag{29}$$

It is therefore observed that Daboczi multi-parameter optimization model [4] is a special case of the generalized multi-parameter deconvolution where $|L_r(k)|^2$ can be progressively used to improve the SNR

of the deconvolved data. Consequently, if needed, we can find $|L_r(k)|^2$ for any r .

In this paper, the following model is used

$$\hat{X}(k) = \frac{Y(k)H^*(k)}{|H(k)|^2 + g|L_1(k)|^2 + x|L_2(k)|^2} \tag{30}$$

This is exactly the model of equation (20) with $q = 2$, $u_0 = 0$, $u_1 = g$ and $u_2 = x$.

The estimated input distribution in Eq. (8) is computed by Fourier transformation which gives

$$\hat{X}(k) = \sum_{i=1}^M B_i e^{j\frac{2fk}{N} \ln \lambda_i} \tag{31}$$

The output of the deconvolution stage will take this form

$$\hat{X}(k) = \sum_{i=1}^M B_i e^{j\frac{2fk}{N} \ln \lambda_i} \tag{32}$$

The original signal $I(\dagger)$ has undergone many manipulations including Gardner transformation, discretization and deconvolution, to arrive at (32). The signal $\hat{X}(k)$ can, therefore, not be stationary. There is, thus, the need to look for a procedure for stationarizing

the signal in (32) such that it would be stationary noise which would make further analysis easier. The method used here is the same as the one used in Jibia & Salami (2012b). The resulting stationary signal is therefore

$$\hat{x}(k) = \sum_{i=1}^M B_i e^{\left(j\frac{2fk}{N_d} \ln \lambda_i\right)} \tag{33}$$

$k = 1, 2, \dots, N_d$; $N_d = 2N_0 + 1$, N_0 is the truncation point.

In addition to the errors introduced due to Gardner transform and accompanying deconvolution, there would always be some external noise. The effect of this noise is

also accommodated as detailed in [9].

The minimum-norm method uses an arbitrary vector

$$d = [d(1) \quad d(2) \quad \dots \quad d(N_d)] \tag{34}$$

Constrained to lie in the noise subspace.

The autocorrelation matrix of \hat{x} may be expressed in terms of its Eigen decomposition as

$$R_{xx} = \sum_{i=1}^P \lambda_i v_i v_i^H = V \Lambda V^H \tag{35}$$

Where Λ is a diagonal matrix of the eigenvalues in descending order on the diagonal ($\lambda_1 \geq \lambda_2 \geq \dots \geq \lambda_P$) while the columns of V are the corresponding eigenvectors. The M largest eigenvalues correspond to the signal and the remaining

eigenvalues ($P - M$) have equal values and correspond to the noise. R_{xx} can thus be partitioned into two portions, one due to the signal and the other due to the noise eigenvectors

$$R_{xx} = V_s \Lambda_s V_s^H + \sigma_w^2 V_w V_w^H \tag{36}$$

where $V_s = [v_1 \ v_2 \ \dots \ v_M]$ and $V_w = [v_{M+1} \ v_{M+2} \ \dots \ v_P]$

are matrices whose columns consists of signal and noise eigenvectors respectively. Λ is an $M \times M$ diagonal matrix containing the signal eigenvalues. Thus the P -dimensional subspace has been broken into two

subspaces, i.e. the so-called signal and noise subspaces.

The matrices that project an arbitrary vector on the signal and noise subspaces are (Manolakis et al, 2005):

$$P_s = V_s V_s^H \text{ and } P_w = V_w V_w^H \tag{37}$$

Thus, for any arbitrary vector that lies in the noise subspace

$$P_w d = d \quad \text{and} \quad P_s d = 0 \tag{38}$$

where $\mathbf{0}$ is the length- M zero vector.

The minimum norm seeks to minimize the norm of d in order to avoid spurious peaks in the pseudo-

spectrum. From equation (17), the norm of a vector d contained in the noise subspace is

$$\|d\|^2 = d^H d = d^H P_w d \tag{39}$$

Since an unconstrained minimization of this norm will produce the zero vector, the first element of b is constrained to be unity, i.e.

$$u_1^H d = 1 \tag{40}$$

The solution to this can be found by using Lagrange multipliers (Manolakis et al, 2005) as

$$b_{mn} = \frac{P_w u_1}{u_1^H P_w u_1} \tag{41}$$

The $\ln \lambda_i$ estimates are then obtained from the peaks in the pseudo-spectrum of the minimum norm vector

SIMULATION RESULTS

In this section, simulation results are presented. The simulations were carried out to investigate the effectiveness of the proposed combination. Three signals are used. A two component signal is used to test resolvability of the method. A five-component high resolution signal is then used to test the ability of this approach to analyze high resolution signals. Finally, an eight component signal is used to demonstrate the efficacy of the method in measuring the lifetime of data consisting of many lifetimes. Although this is not

$$I_1(t) = 0.1e^{-0.1t} + 0.2e^{-0.2t} + n(t) \tag{42}$$

The distribution function of this signal

$$x_1(t) = 0.1^{(1-r)}u(t - \ln 10) + 0.2^{(1-r)}u(t - \ln 5) \tag{43}$$

Noise was added using the MATLAB function *awgn*. Nonlinear change of variables (i.e. the Gardner transform) was performed by multiplying $I_1(t)$ by e^{rt} . The discrete form of equation (6) was obtained by selecting $r = 1$, $\Delta t = 0.25$, $n_{\max} = 44$, $n_{\min} = -83$. The DFT of equation (9) was therefore computed using FFT with $N = 128$. Table 1 shows the results of applying the proposed combination. Selected pseudo spectra over low ($SNR \leq 40dB$), medium ($40dB < SNR < 100dB$) and high ($SNR \geq 100dB$) SNRs are shown in Figure. For the purpose of comparison, DFT plots are shown (broken lines) along with the actual plot (solid). The DFT graphs are obtained by windowing the deconvolved data to

available in practice, it is possible in simulation.

For the purpose of simulation, an additive white Gaussian noise $n(t)$ is introduced to all the synthesized signals. The signal to noise ratio (SNR) is varied by varying the level of noise.

A. Resolvability of the components

To determine the effectiveness of the proposed combination in analyzing basic signals, the following 2-component signal was used:

remove high frequency noise and then inverse transforming, instead of using any of the three modeling techniques proposed in this thesis. The pseudo spectrum was plotted against negative time in order to arrange the exponents in ascending order on the horizontal axis. This means the first peak occurs at $-\ln 10 = -2.3025$ and the last at $-\ln 5 = -1.6094$. The values of P is $2M + 1$ respectively. The useful length of the deconvolved data was selected to be $N_0 = 10$. This is based on the results presented by Jibia & Salami (2012b).

These settings are also used for the two other signals analyzed next.

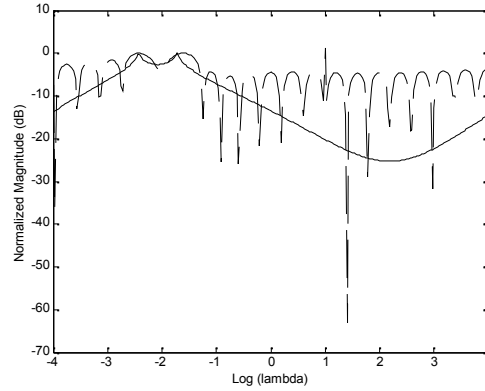


Figure 1. Minimum norm (with MPD) pseudo spectrum for $I_1(t)$ at low SNR

Table 1: Estimated log of decay rates ($\ln \lambda_i$) for $I_1(t)$

Expected Value	LOW SNR	MEDIUM SNR	HIGH SNR
-2.3025	-2.313	-2.438	-2.428
-1.6094	-1.563	-1.688	-1.522

B. Analysis of a High-Resolution Signal

The following signal was used to test the effectiveness of the proposed combination in resolving a high resolution signal.

$$I_2(t) = 0.5e^{-0.5t} + e^{-t} + 2e^{-2t} + 5e^{-5t} + 10e^{-10t} + n(t) \tag{44}$$

It is noteworthy that for this signal; $\frac{\lambda_1}{\lambda_2} = \frac{\lambda_2}{\lambda_3} = \frac{\lambda_4}{\lambda_5} = \frac{1}{2}$.

The distribution function for the signal $I_2(t)$ is as follows:

$$x_2(t) = 0.5^{(1-r)}u(t - \ln 2) + u(t) + 2^{(1-r)}u(t + \ln 2) + 5^{(1-r)}u(t + \ln 5) + 10^{(1-r)}u(t + \ln 10) \tag{45}$$

The result of applying the proposed combination on $I_2(t)$ is shown in Table 2. Figure 2 shows a typical pseudo spectrum for this signal.

Table 2: Estimated log of decay rates (ln λ_i) for $I_2(\ddagger)$

Expected Value	LOW SNR	MEDIUM SNR	HIGH SNR
-0.6931	-0.8750	-0.8750	-0.7500
0	-0.0312	-0.0938	0.1250
0.6931	0.8125	0.8438	0.9688
1.6094	1.6888	1.8440	1.8440
2.3025	2.5940	2.6880	2.7190

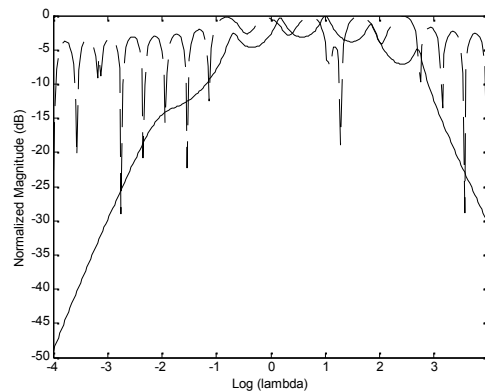


Figure 2. Minimum norm (with MPD) pseudo spectrum for $I_2(\ddagger)$ at medium SNR

C. Analyzing Signals with Large Number of Components

Also tested is the ability of the combination to resolve large number of components of diversified magnitude. To achieve that, the following signal is used:

$$\begin{aligned}
 I_3(\ddagger) = & 0.01e^{-0.01\ddagger} + 0.025e^{-0.025\ddagger} \\
 & + 0.05e^{-0.05\ddagger} + 0.1e^{-0.1\ddagger} + 0.5e^{-0.5\ddagger} \\
 & + 2e^{-2\ddagger} + 10e^{-10\ddagger} + 25e^{-25\ddagger} + n(\ddagger)
 \end{aligned} \tag{46}$$

The distribution function for this signal is

$$\begin{aligned}
 x_3(t) = & 0.01^{(t-r)}u(1 - \ln 100) + 0.025^{(t-r)}u(1 - \ln 40) + 0.1^{(t-r)}u(1 - \ln 20) \\
 & + 0.1^{t-r}u(1 - \ln 10) + 0.5^{(t-r)}u(1 - \ln 2) + 2^{(t-r)}u(1 + \ln 2) \\
 & + 10^{(t-r)}u(1 + \ln 10) + 25^{(t-r)}u(1 + \ln 25)
 \end{aligned} \tag{47}$$

Table 3 shows the result of applying our combination to this signal. All the components are detected over high SNR, but poor results are obtained over low and medium

SNRs. A typical pseudo-spectrum for this signal is shown in Figure 3.

Table 3: Estimated log of decay rates (ln λ_i) for $I_2(\ddagger)$

Expected Value	LOW SNR	MEDIUM SNR	HIGH SNR
-4.6052	-4.313	-4.402	-4.2500
-3.6888	-3.656	-3.6021	-3.5630
-2.9957	-2.813	-2.810	-2.8440
-2.3025	-1.406	-1.31	-0.9063
-0.6931	-0.314	0.2188	0.0937
0.6931	0.902	2.1880	2.0630
2.3025	2.565	2.3025	2.8440
3.2188	3.688	3.25	3.5310

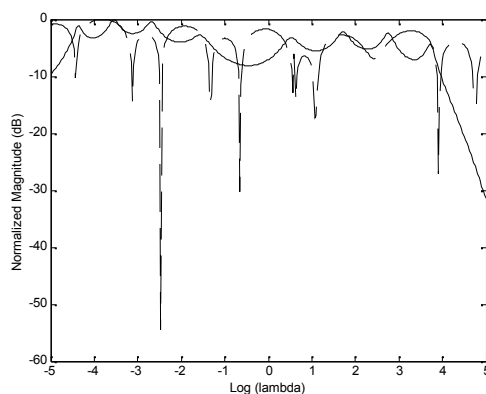


Figure 3. Minimum norm (with MPD) pseudo-spectrum for $I_3(\ddagger)$ at high SNR

EXPERIMENTAL RESULTS

Combination of minimum norm and MPD was used to post-process real data obtained from fluorescence decay experiment. Two fluorophores were used, viz. acridine orange ($C_{17}H_{12}ClN_3$) and Fluorescein Sodium ($C_{20}H_{10}Na_2O_5$). The experimental setup is as in Jibia & Salami (2012c).

The eigenvector algorithms were applied to the data in

a similar manner done in the simulation and was selected to be 0.5. The deconvolution parameters selected are for medium range of the SNR. The sampling interval was $\Delta t = 0.25, n_{max} = 44$, making $N = 128$. Table 4 shows the result of data analysis. The corresponding pseudo-spectra are shown in Figures 4 through 6.

Table 4: Estimated log of decay rates ($\ln \lambda_i$) from fluorescence decay experiments.

Mixture	Expected value	Log estimates	Percentage deviation
Acridine orange	0.5978	0.7188	20.24
Fluorescein Sodium	-1.4584	-1.375	5.72
Acridine Orange +Fluorescein Sodium	0.6539	0.625	4.42
	-1.4584	-1.469	0.73

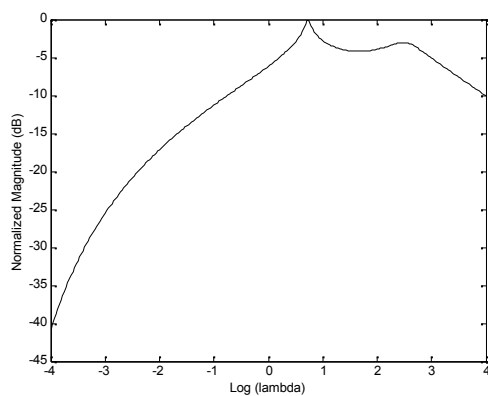


Figure 4. Minimum norm (with MPD) pseudospectrum for Acridine Orange in water

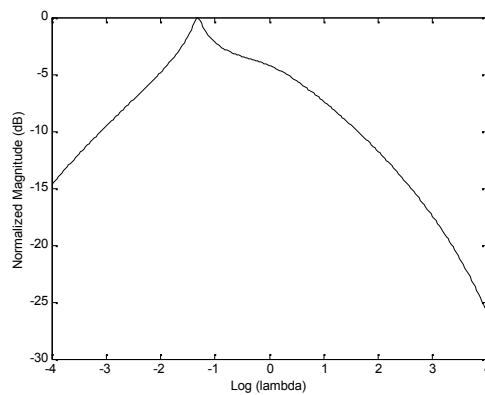


Figure 5. Minimum norm (with MPD) pseudospectrum for Fluorescein Sodium in water

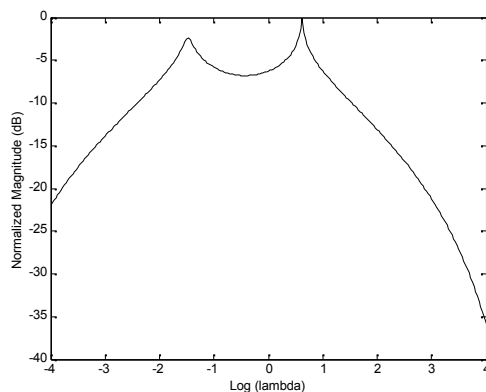


Figure 6. Minimum norm (with MPD) pseudo-spectrum for Fluorescein Sodium + Acridine Orange in water

A close look at the Figures and the table reveals that although its pseudo-spectra is noisy, the combination of MPD and MN is capable of giving near accurate estimates of decay rates. However, some spurious peaks are observed for single fluorophores like the pseudo-spectrum of Acridine orange shown in Figure 4.

CONCLUSION

In this paper, a new approach for the measurement of fluorescence lifetimes has been introduced. The approach consists of a combination of multi-parameter deconvolution and minimum norm is used to post-process the data resulting from the application of Gardner transform to fluorescence decay data. Further research may explain ways of fine-tuning the approach so as to avoid spurious peaks when analyzing data involving only one fluorophore.

REFERENCES

Isernberg, I. (1983). Robust estimation in pulse fluorometry: A study of the method of moments and least squares. *The Biophysical Journal*, 43 (2), 141-148.

Isernberg, I., & Dyson, R. D. (1969). The analysis of fluorescence decay by a method of moments. *The Biophysical Journal*, 9(11), 1337-1350.

Istratov, A.A. & Vyvenko, O.F. (1999) Exponential Analysis in Physical Phenomena. *Review of Scientific Instruments*, 70 (2), pp. 1233-1257.

Jibia, A. U. & Salami, M. J. E. (2007). Performance Evaluation of MUSIC and Minimum Norm Eigenvector Algorithms in Resolving Noisy Multiexponential Signals. *International Journal of Computer Science*, 2 (4), pp. 235- 239.

Jibia, A. U., Salami, M. J. E. & Khalifa, O. O. (2008). Effect of Multiple Deconvolution Parameters on the Resolvability of Decay Rates of Multiexponential Signals. *Proceedings of 15th International Conference on Systems, Signals and Image Processing (IWSSIP 2008) Bratislava*, pp. 347 - 350.

Jibia, A.U. & Salami, M.J.E. (2012a). An Appraisal of Gardner Transform-Based Methods of Transient Multiexponential Signal Analysis. *International Journal of Computer Theory and Engineering*, 4 (1): 16-25.

Jibia, A.U. & Salami, M.J.E. (2012b). Transient Multiexponential Data Selection Using Cramer-Rao

Lower Bound. *Proc. International Conference on Computer and Automation Engineering, Mumbai, Janua* pp. 227-232.

- Jibia, A.U. & Salami, M.J.E. (2012c). Analysis of transient multi-exponential signals using exponential compensation deconvolution. *Measurement* 45, pp. 19-29.
- Jibia, A.U., Salami, M.J.E. & Khalifa, D.D. (2010). Effect of Sampling on the Parameter Estimates of

Multicomponent Transients. *2nd International Conference on Computer and Automation Engineering, Singapore*. 5, pp 704-708.

- Lakowicz, J. R. (2006). *Principles of Fluorescence Spectroscopy*, 3rd Edition. Springer Science and Business Media, LLC, Singapore.
- Manolakis, D.G., Ingle, V.K. & Kogon, S.M. (2005) *Statistical and adaptive signal processing*, Artech House, Inc., Norwood.